**Proceedings of the 7th GACM Colloquium on Computational Mechanics
for Young Scientists from Academia and Industry
October 11-13, 2017 in Stuttgart, Germany**

Two-scale anisotropic damage modeling of SMC

Johannes Görthofer[1]*, Malte Schemmann[1] and Thomas Böhlke[1]

Micro Abstract
We present a two-scale anisotropic damage model that captures matrix damage and fiber-matrix interface debonding. Based on the fiber orientation distribution and a Weibull probability distribution of the interface strength, the damage evolution on the microscale is determined. Within this work focus lies on the comparison of different matrix damage evolution models. To predict the macroscopic behavior, a mean field homogenization with the Mori-Tanaka method based on orientation tensors of second and fourth order is applied.

[1]Institute of Engineering Mechanics, Chair for Continuum Mechanics, Karlsruhe Institute of Technology (KIT), Germany

***Corresponding author**: johannes.goerthofer@kit.edu

Introduction

Due to their high lightweight potential, economical mass-production and excellent formability, discontinuous fiber reinforced composites are increasingly used for load-carrying components in the automotive sector. The material class under consideration is SMC (sheet molding compound), a thermoset matrix reinforced with glass fibers. The orientation distribution of the fibers in this material is highly heterogeneous and anisotropic in a process sensitive way.

Damage in polymer matrix composites derives from the following three phenomena: matrix (M) damage, fiber (F) breakage and fiber-matrix interface (I) debonding. Various authors [14], [11], [6], [2] showed that fiber breakage can be neglected within the contemplation of SMC. Typically damage evolution initiates at fiber matrix interfaces and propagates between the interfaces in the form of matrix cracks.

The aim of this work is the development of a micromechanical model which captures matrix damage and interface debonding to predict the macroscopic behavior of discontinuous fiber reinforced polymers. The effective stiffness is obtained by a Mori-Tanaka (MT) [15] homogenization scheme. The model is based on a purely elasto-damage behavior.

After an overview of the MT mean field homogenization scheme using fiber orientation information, the focus in this study lies on different matrix damage evolution models. A short outlook on an interface damage model including a Weibull probability distribution of the interface strength is given afterwards.

Fiber Orientation Distribution

The microstructural information on how the fibers are oriented within the composite can be represented approximately by the fiber orientation distribution function (FODF) $f(\boldsymbol{n})$ which is defined as

$$\frac{\mathrm{d}v}{v}(\boldsymbol{n}) = f(\boldsymbol{n})\,\mathrm{d}S. \tag{1}$$

Here, $\mathrm{d}S$ is the surface element on the unit sphere $S := \{\boldsymbol{n} \in \mathbb{R}^3 : \|\boldsymbol{n}\| = 1\}$. The FODF describes the volume fraction $\mathrm{d}v/v$ of fibers with orientiation $\boldsymbol{n}$ with respect to all fibers [18], [16]. The

FODF is non-negative, normalized and symmetric

$$f(\boldsymbol{n}) \geq 0, \quad \int_S f(\boldsymbol{n})\,\mathrm{d}S = 1, \quad f(\boldsymbol{n}) = f(-\boldsymbol{n}), \quad \forall \boldsymbol{n} \in S. \tag{2}$$

An empirical representation of the FODF, based on m different directions $\boldsymbol{n}_\beta$ with corresponding weights $c\,(\boldsymbol{n}_\beta)$, is given through

$$f(\boldsymbol{n}) = \sum_{\beta=1}^{m} c\,(\boldsymbol{n}_\beta)\,\delta(\boldsymbol{n}, \boldsymbol{n}_\beta), \tag{3}$$

with $\delta(\boldsymbol{n}, \boldsymbol{n}_\beta)$ being a Dirac distribution. The weights $c\,(\boldsymbol{n}_\beta)$ can be interpreted as the fraction of fibers oriented in the direction $\boldsymbol{n}_\beta$. Based on the FODF, it is possible to derive fiber orientation tensors (FOT) [1, 12]. The so called fabric tensors of 2^{nd}, 4^{th} and k^{th} order can be calculated as

$$\boldsymbol{N} = \int_S f(\boldsymbol{n})\boldsymbol{n}^{\otimes 2}\,\mathrm{d}S, \quad \mathbb{N} = \int_S f(\boldsymbol{n})\boldsymbol{n}^{\otimes 4}\,\mathrm{d}S, \quad \mathbb{N}_{\langle k \rangle} = \int_S f(\boldsymbol{n})\boldsymbol{n}^{\otimes k}\,\mathrm{d}S, \tag{4}$$

with the abbreviations

$$\boldsymbol{n}^{\otimes 2} = \boldsymbol{n} \otimes \boldsymbol{n}, \quad \boldsymbol{n}^{\otimes 4} = \boldsymbol{n} \otimes \boldsymbol{n} \otimes \boldsymbol{n} \otimes \boldsymbol{n}, \quad \boldsymbol{n}^{\otimes k} = \underbrace{\boldsymbol{n} \otimes \boldsymbol{n} \otimes \cdots \otimes \boldsymbol{n}}_{k \text{ times}}. \tag{5}$$

For an empirical FODF, according to equation (3), this leads to

$$\mathbb{N}_{\langle k \rangle} = \sum_{\beta=1}^{m} c\,(\boldsymbol{n}_\beta)\,\boldsymbol{n}_\beta^{\otimes k}. \tag{6}$$

Further representations of FOTs can, e.g., be found in [12].

Effective Linear Elastic Behavior

The effective stiffness $\bar{\mathbb{C}}$ couples the effective stress $\bar{\boldsymbol{\sigma}}$ and the effective strain $\bar{\boldsymbol{\varepsilon}}$ as

$$\bar{\boldsymbol{\sigma}} = \bar{\mathbb{C}}[\bar{\boldsymbol{\varepsilon}}]. \tag{7}$$

Based on the MT assumption that the fiber strain localization $\mathbb{A}_{\mathrm{F}}^{\mathrm{SIP}}$ relates the phase-averaged fiber (F) strain $\boldsymbol{\varepsilon}_{\mathrm{F}}$ to the phase-averaged matrix (M) strain $\boldsymbol{\varepsilon}_{\mathrm{M}}$ in the way that $\boldsymbol{\varepsilon}_{\mathrm{F}} = \mathbb{A}_{\mathrm{F}}^{\mathrm{SIP}}\,[\boldsymbol{\varepsilon}_{\mathrm{M}}]$, the effective stiffness then is calcuted via

$$\bar{\mathbb{C}} = \mathbb{C}_{\mathrm{M}} + c_{\mathrm{F}}\langle(\mathbb{C}_{\mathrm{F}} - \mathbb{C}_{\mathrm{M}})\,\mathbb{A}_{\mathrm{F}}^{\mathrm{MT}}\rangle_{\mathrm{F}}. \tag{8}$$

Hereby, $\mathbb{C}_{\mathrm{M}}$, $\mathbb{C}_{\mathrm{F}}$ and c_{F} are the matrix and fiber stiffness and the fiber volume fraction, respectively. The fiber strain localization $\mathbb{A}_{\mathrm{F}}^{\mathrm{SIP}}$ based on the single inclusion problem (SIP) formulated by Eshelby [5] is

$$\mathbb{A}_{\mathrm{F}}^{\mathrm{SIP}} = \left(\mathbb{I}^{\mathsf{S}} + \mathbb{P}_0\,(\mathbb{C}_{\mathrm{F}} - \mathbb{C}_{\mathrm{M}})\right)^{-1}, \tag{9}$$

with $\mathbb{I}^{\mathsf{S}}$ being the 4^{th} order identity on symmetric tensors. An explicit formulation of the symmetric polarization tensor $\mathbb{P}_0$ can be found in [3]. Furthermore, the MT fiber strain localization $\mathbb{A}_{\mathrm{F}}^{\mathrm{MT}}$ and matrix strain localization $\mathbb{A}_{\mathrm{M}}^{\mathrm{MT}}$ are

$$\mathbb{A}_{\mathrm{F}}^{\mathrm{MT}} = \mathbb{A}_{\mathrm{F}}^{\mathrm{SIP}}\mathbb{A}_{\mathrm{M}}^{\mathrm{MT}}, \quad \mathbb{A}_{\mathrm{M}}^{\mathrm{MT}} = \left(c_{\mathrm{M}}\mathbb{I}^{\mathsf{S}} + c_{\mathrm{F}}\langle\mathbb{A}_{\mathrm{F}}^{\mathrm{SIP}}\rangle_{\mathrm{F}}\right)^{-1}. \tag{10}$$

The matrix volume fraction is given by $c_{\mathrm{M}} = 1 - c_{\mathrm{F}}$. In case of a transversally isotropic and symmetric tensor $\mathbb{A}$ with symmetry axis in $\boldsymbol{e}_1$-direction, an analytical formulation of the orientation average over all fibers $\langle\mathbb{A}\rangle_{\mathrm{F}}$ in dependence of a 2^{nd} and 4^{th} order FOT, $\boldsymbol{N}$ and $\mathbb{N}$, is given by [1] as

$$\begin{aligned}
\langle\mathbb{A}\rangle_{\mathrm{F}} \quad = \quad & b_1\mathbb{N} + b_2(\boldsymbol{N} \otimes \boldsymbol{I} + \boldsymbol{I} \otimes \boldsymbol{N}) \\
& + b_3(\boldsymbol{N}\Box\boldsymbol{I} + (\boldsymbol{N}\Box\boldsymbol{I})^{\mathsf{T_R}} + (\boldsymbol{I}\Box\boldsymbol{N})^{\mathsf{T_H}} + (\boldsymbol{I}\Box\boldsymbol{N})^{\mathsf{T_R}}) \\
& + b_4\boldsymbol{I} \otimes \boldsymbol{I} + b_5\mathbb{I}^{\mathsf{S}}.
\end{aligned} \tag{11}$$

The coefficients b_1 to b_5 are specific parameters corresponding to $\mathbb{A}$.

Orientation Dependent Stress Localization

The localized phase-averaged stresses within the matrix $\boldsymbol{\sigma}_{\mathrm{M}}$ and the fibers $\boldsymbol{\sigma}_{\mathrm{F}}$ can be calculated with the MT stress localization tensors $\mathbb{B}_{\mathrm{M}}^{\mathrm{MT}}$ and $\mathbb{B}_{\mathrm{F}}^{\mathrm{MT}}$

$$\boldsymbol{\sigma}_{\mathrm{M}} = \mathbb{B}_{\mathrm{M}}^{\mathrm{MT}}[\overline{\boldsymbol{\sigma}}], \qquad \boldsymbol{\sigma}_{\mathrm{F}} = \mathbb{B}_{\mathrm{F}}^{\mathrm{MT}}[\overline{\boldsymbol{\sigma}}]. \tag{12}$$

Hereby, we have

$$\mathbb{B}_{\mathrm{M}}^{\mathrm{MT}} = \left(c_{\mathrm{M}}\mathbb{I}^{\mathsf{S}} + c_{\mathrm{F}}\langle\mathbb{B}_{\mathrm{F}}^{\mathrm{SIP}}\rangle_{\mathrm{F}}\right)^{-1}, \qquad \mathbb{B}_{\mathrm{F}}^{\mathrm{MT}} = \langle\mathbb{B}_{\mathrm{F}}^{\mathrm{SIP}}\rangle_{\mathrm{F}}\mathbb{B}_{\mathrm{M}}^{\mathrm{MT}}. \tag{13}$$

The fiber stress localization tensor in the single inclusion problem $\mathbb{B}_{\mathrm{F}}^{\mathrm{SIP}}$ [5] is given by

$$\mathbb{B}_{\mathrm{F}}^{\mathrm{SIP}} = \left(\mathbb{I}^{\mathsf{S}} + \mathbb{C}_{\mathrm{M}}\left(\mathbb{I}^{\mathsf{S}} - \mathbb{P}_0\mathbb{C}_{\mathrm{M}}\right)\left(\mathbb{C}_{\mathrm{F}}^{-1} - \mathbb{C}_{\mathrm{M}}^{-1}\right)\right)^{-1}, \tag{14}$$

with the inclusion being oriented in $\boldsymbol{e}_1$-direction. According to [4], the fiber stress $\boldsymbol{\sigma}_{\mathrm{F}}^{\angle}(\boldsymbol{n})$ in any fiber orientation $\boldsymbol{n}$ can be calculated from the macroscopic stress $\bar{\boldsymbol{\sigma}}$ using

$$\boldsymbol{\sigma}_{\mathrm{F}}^{\angle}(\boldsymbol{n}) = \mathbb{B}_{\mathrm{F}}^{\mathrm{SIP}\angle}(\boldsymbol{n})\,\mathbb{B}_{\mathrm{M}}^{\mathrm{MT}}[\overline{\boldsymbol{\sigma}}] \quad \text{with} \quad \mathbb{B}_{\mathrm{F}}^{\mathrm{SIP}\angle}(\boldsymbol{n}) = \boldsymbol{Q}(\boldsymbol{n}) \star \mathbb{B}_{\mathrm{F}}^{\mathrm{SIP}},\ \boldsymbol{Q} \in Orth. \tag{15}$$

Matrix Damage

The matrix is modeled based on its phase-averaged behavior. A comparison of different matrix damage evolution models is conducted. A rate dependent isotropic damage model based on a power law evolution is compared to a rate independent anisotropic damage model based on an energy formulation developed by Govindjee et al. [9].

Isotropic Damage Model

Based on a scalar damage variable $\alpha \in [0,1)$ [17] and the initial undamaged stiffness $\mathbb{C}_0$, the elastic storage energy is introduced as

$$W(\boldsymbol{\varepsilon}, \alpha) = \frac{1}{2}(1-\alpha)\boldsymbol{\varepsilon} \cdot \mathbb{C}_0[\boldsymbol{\varepsilon}], \tag{16}$$

which leads to a damaged stiffness $\mathbb{C}$ of

$$\mathbb{C} = (1-\alpha)\,\mathbb{C}_0. \tag{17}$$

The damage variable α can be interpreted as crack density in an isotropic matrix (see, e.g., [10]). A power law ansatz for the damage evolution based on the conjugated strain energy β is assumed

$$\dot{\alpha} = \dot{\alpha}_0\left(\frac{\beta}{\beta_0}\right)^m = \dot{\alpha}_0\left(\frac{\boldsymbol{\varepsilon}\cdot\mathbb{C}_0[\boldsymbol{\varepsilon}]}{2\beta_0}\right)^m = \dot{\alpha}_0\left(\frac{\boldsymbol{\sigma}\cdot\mathbb{S}_0[\boldsymbol{\sigma}]}{2\beta_0(1-\alpha)^2}\right)^m. \tag{18}$$

Hereby, $\dot{\alpha}_0$, β_0 and m are material parameters and $\mathbb{S}_0 = \mathbb{C}_0^{-1}$ is the compliance tensor. The model leads to a strain rate dependent behavior of the damage and stress evolution under unaxial loading, as depicted in Fig. 1. The damage variable α increases exponentially, while the stress-strain behavior intrinsically shows a softening behavior due to equation (17). Accordingly, the softening behavior is smooth.

Anisotropic Damage Model

An anisotropic damage evolution model according to Govindjee et al. [9] based on three damage functions $\Phi_k(\beta, \boldsymbol{\sigma})$ is examined. The elastic storage energy is superposed of an elastic energy and an energy $p(\alpha)$ due to the accumulated damage α given by

$$W(\boldsymbol{\varepsilon}, \mathbb{C}, \alpha) = \frac{1}{2}\boldsymbol{\varepsilon}\cdot\mathbb{C}[\boldsymbol{\varepsilon}] + p(\alpha), \tag{19}$$

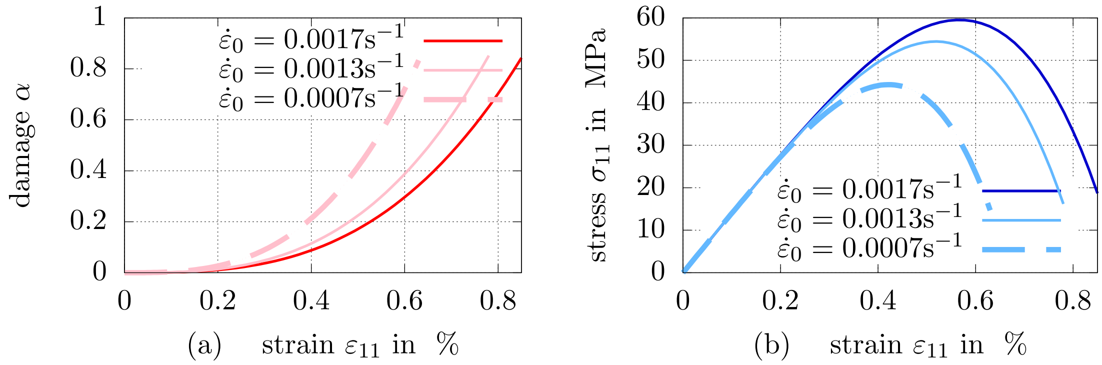

Figure 1. Rate dependent material behavior - isotropic damage law

with the stiffness $\mathbb{C}$ itself being considered an internal variable. Hereby, the evolution of the accumulated damage α and the compliance $\mathbb{S}$ are

$$\dot{\alpha} = \sum_{k=1}^{3} \gamma_k \left(\partial_\beta \Phi_k\right) \quad \text{and} \quad \dot{\mathbb{S}} = \sum_{k=1}^{3} \gamma_k \left(\frac{\partial_\sigma \Phi_k \otimes \partial_\sigma \Phi_k}{\partial_\sigma \Phi_k \cdot \boldsymbol{\sigma}} \right). \tag{20}$$

The conjugated driving force β is defined as

$$\beta\left(\alpha\right) = -\frac{\partial W(\boldsymbol{\varepsilon}, \mathbb{C}, \alpha)}{\partial \alpha} = -\frac{\partial p(\alpha)}{\partial \alpha}, \tag{21}$$

and describes the material behavior under loading. The function $\beta\left(\alpha\right)$ governs the damage behavior and can be used to model a strain hardening or a strain softening behavior. Due to the ill-posedness of the boundary value problem, a viscous regularization is necessary when considering strain softening (see, e.g., [8]). Describing the latter by $\beta\left(\alpha\right) = g_t\left(1 - \exp\left(-H\alpha\right)\right)$, with g_t and H being material parameters, leads to a behavior under uniaxial loading as shown in Fig. 2. Theoretically, the accumulated damage variable $\alpha \in [0, \infty)$ can take any non-negative

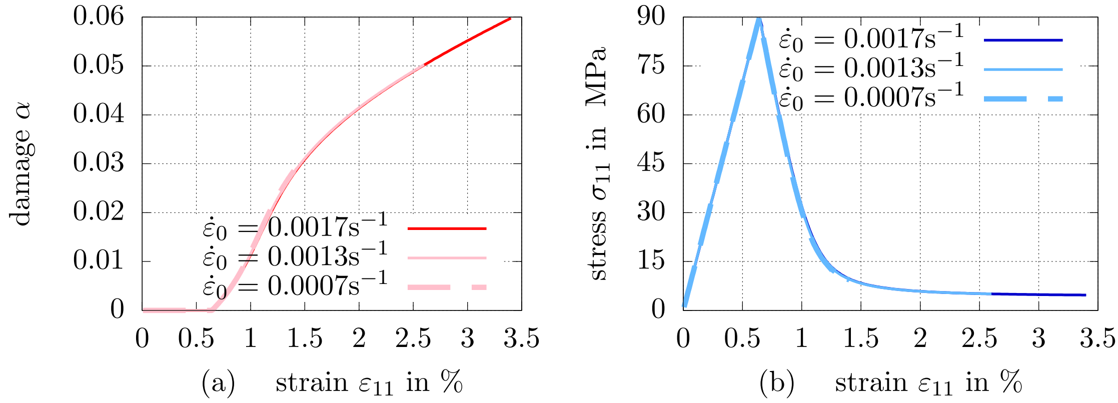

Figure 2. Rate independent strain softening material behavior - anisotropic damage law

value, but is - depending on the chosen material parameters - usually quite small (as can be seen in Fig.2(a)). Unlike the discussed isotropic damage model, the evolution of α within the anisotropic damage model does not follow an exponential course. Furthermore, in contrast to the isotropic damage model, where no seperate softening law has to be included, in the anisotropic damage model the softening behavior is triggered through a maximal bearable stress g_t. As soon as damage occurs, the stress-strain curve exponentially decreases in a non-differentiable way. Depending on the number of employed damage functions Φ_k, the model behavior can be further adjusted to the behavior of the matrix material.

Young's Modulus Evolution

Young's Modulus can be evaluated in any arbitrary direction $\boldsymbol{n}$ parametrized as polar coordinates by two angles ϑ and φ. A depiction of the directional Young's Modulus evolution within the $x-y-$plane ($\vartheta = \pi/2$), with x being the abscissa and unaxial loading axis can be seen in Fig. 3. Both planar plots are rotationally symmetric with respect to the $x-$axis. The isotropic law (a)

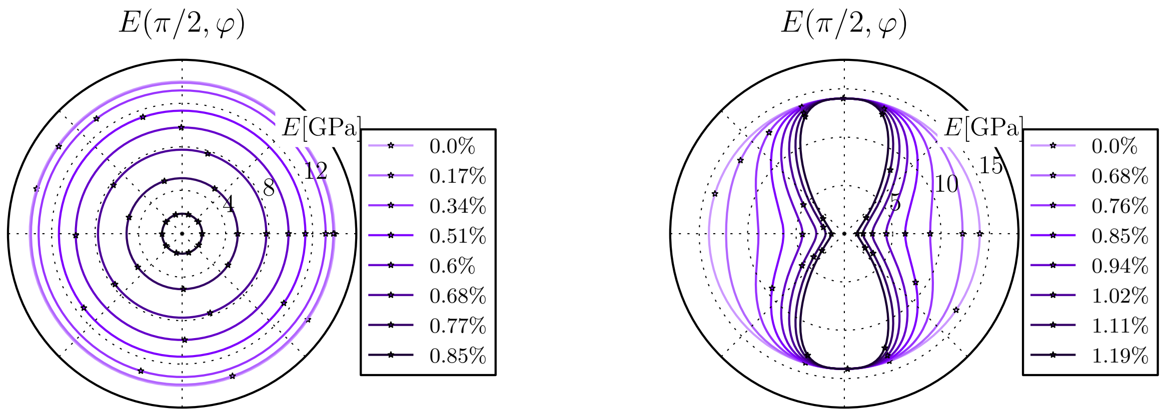

(a) isotropic damage law

(b) anisotropic damage law

Figure 3. Young's Modulus plot $x-y-$plane, uniaxial loading in $x-$direction

predicts an isotropic reduction of the stiffness independent of the actual loading case, whereas the stiffness reduction of the anisotropic law (b) is highest in loading direction. Perpendicular to the loading direction stiffness remains constant. Due to the occurence of damage, the material behavior changes therefore, from isotropic to transversally isotropic.

Interface Damage

Using the fiber orientation information provided by the FODF or FOT respectively, an equivalent interface stress in each fiber direction $\boldsymbol{n}$ can be calculated (see, e.g., [7]). Analogously to [13], the interface strength is assumed to be Weibull distributed. A comparison of the fraction of fibers in a specific direction $\boldsymbol{n}$ and the probability of fibers surviving the current load, yields a damage evolution criterion.

Conclusions

To describe the matrix behavior, various damage evolution models are available. An adaption to catch strain softening as well as strain hardening has already been implemented. Viscous regularization is applied when necessary. The interface model needs to capture the stress driven damage evolution due to an exceed of the interface strength depending on the loading.

In the development of the damage models on the microscale, it is necessary to ensure that the basic assumptions of the considered MT homogenization scheme are not violated. A suitable combination of a matrix and an interface damage model is necessary in order to correctly and efficiently predict the macroscopic behavior.

Acknowledgements

We acknowledge the financial support by the German Research Foundation (DFG) within the International Research Training Group "Integrated engineering of continuous-discontinuous long fiber reinforced polymer structures" (GRK 2078).

References

[1] S. G. Advani and C. L. Tucker III. The Use of Tensors to Describe and Predict Fiber Orientation in Short Fiber Composites. *Journal of Rheology*, 31(8):751–784, 1987.

[2] A. Ben Cheikh Larbi, K. Sai, H. Sidhom, and D. Baptiste. Constitutive Model of Micromechanical Damage to Predict Reduction in Stiffness of a Fatigued SMC Composite. *Journal of Materials Engineering and Performance*, 15(5):575–580, 2006.

[3] P. P. Castaneda and P. Suquet. Nonlinear Composites. *Advances in Applied Mechanics*, 34(12):172–195, 1998.

[4] D. Duschlbauer, H. E. Pettermann, and H. J. Böhm. Mori-Tanaka based evaluation of inclusion stresses in composites with nonaligned reinforcements. *Scripta Materialia*, 48(3):223–228, 2003.

[5] J. Eshelby. The determination of the elastic field of an ellipsoidal inclusion and related problems. *Proceedings of the Royal Society of London. Series A, Mathematical and Physical Sciences*, 241(1226):376–396, 1957.

[6] J. Fitoussi, M. Bocquet, and F. Meraghni. Effect of the matrix behavior on the damage of ethylene-propylene glass fiber reinforced composite subjected to high strain rate tension. *Composites Part B: Engineering*, 45(1):1181–1191, 2013.

[7] J. Fitoussi, G. Guo, and D. Baptiste. A statistical micromechanical model of anisotropic damage for S.M.C. composites. *Composites Science and Technology*, 58(5):759–763, 1998.

[8] S. Forest and E. Lorentz. Chapter XI: Localization Phenomena and Regularization Methods. In *Local approach to fracture*, pages 311–372. 2004.

[9] S. Govindjee, G. J. Kay, and J. C. Simo. Anisotropic modelling and numerical simulation of brittle damage in concrete. *International Journal for Numerical Methods in Engineering*, 38(361), 1995.

[10] D. Gross and T. Seelig. *Bruchmechanik - Mit einer Einführung in die Mikromechanik*. Springer Berlin Heidelberg, 2011.

[11] Z. Jendli, F. Meraghni, J. Fitoussi, and D. Baptiste. Micromechanical analysis of strain rate effect on damage evolution in sheet molding compound composites. *Composites Part A: Applied Science and Manufacturing*, 35(7-8):779–785, 2004.

[12] K.-I. Kanatani. Distribution of directional data and fabric tensors. *International Journal of Engineering Science*, 22(2):149–164, 1984.

[13] H. K. Lee and S. Simunovic. A damage constitutive model of progressive debonding in aligned discontinuous fiber composites. *International Journal of Solids and Structures*, 38(5):875–895, 2001.

[14] F. Meraghni and M. L. Benzeggagh. Micromechanical modelling of matrix degradation in randomly oriented discontinuous-fibre composites. *Composites Science and Technology*, 55(2):171–186, 1995.

[15] T. Mori and K. Tanaka. Average stress in matrix and average elastic energy of materials with misfitting inclusions. *Acta Metallurgica*, 21(5):571–574, 1973.

[16] V. Müller and T. Böhlke. Prediction of effective elastic properties of fiber reinforced composites using fiber orientation tensors. *Composites Science and Technology*, 130:36–45, 2016.

[17] J. C. Simo and J. W. Ju. Strain- and stress-based continuum damage models-I. Formulation. *International Journal of Solids and Structures*, 23(7):821–840, 1987.

[18] Q. S. Zheng and D. X. Du. An explicit and universally applicable estimate for the effective properties of multiphase composites which accounts for inclusion distribution. *Journal of the Mechanics and Physics of Solids*, 49:2765–2788, 2001.